AGU PUBLICATIONS

Geophysical Research Letters

RESEARCH LETTER
10.1002/2015GL063046

Key Points:
- Fully coupled ecosystem model for California juvenile Chinook salmon
- Favorable salmon growth conditions determined by early season upwelling
- Late spring emigration leads to higher weight gains during first period at sea

Supporting Information:
- Text S1 and Table S1

Correspondence to:
J. Fiechter,
fiechter@ucsc.edu

Citation:
Fiechter, J., D. D. Huff, B. T. Martin, D. W. Jackson, C. A. Edwards, K. A. Rose, E. N. Curchitser, K. S. Hedstrom, S. T. Lindley, and B. K. Wells (2015), Environmental conditions impacting juvenile Chinook salmon growth off central California: An ecosystem model analysis, *Geophys. Res. Lett.*, *42*, 2910–2917, doi:10.1002/2015GL063046.

Received 6 JAN 2015
Accepted 26 MAR 2015
Accepted article online 31 MAR 2015
Published online 23 APR 2015

Environmental conditions impacting juvenile Chinook salmon growth off central California: An ecosystem model analysis

J. Fiechter[1], D. D. Huff[1,2], B. T. Martin[3], D. W. Jackson[2], C. A. Edwards[4], K. A. Rose[5], E. N. Curchitser[6], K. S. Hedstrom[7], S. T. Lindley[2], and B. K. Wells[2]

[1]Institute of Marine Sciences, University of California, Santa Cruz, California, USA, [2]Fisheries Ecology Division, NOAA SWFSC, Santa Cruz, California, USA, [3]Department of Ecology, Evolution, and Marine Biology, University of California, Santa Barbara, California, USA, [4]Ocean Sciences Department, University of California, Santa Cruz, California, USA, [5]Department of Oceanography and Coastal Sciences, Louisiana State University and A&M College, Baton Rouge, Louisiana, USA, [6]Department of Environmental Sciences and Institute of Marine and Coastal Sciences, Rutgers University, New Brunswick, New Jersey, USA, [7]Institute of Marine Science, University of Alaska, Fairbanks, Alaska, USA

Abstract A fully coupled ecosystem model is used to identify the effects of environmental conditions and upwelling variability on growth of juvenile Chinook salmon in central California coastal waters. The ecosystem model framework consists of an ocean circulation submodel, a biogeochemical submodel, and an individual-based submodel for salmon. Simulation results indicate that years favorable for juvenile salmon growth off central California are characterized by particularly intense early season upwelling (i.e., March through May), leading to enhanced krill concentrations during summer near the location of ocean entry (i.e., Gulf of the Farallones). Seasonally averaged growth rates in the model are generally consistent with observed values and suggest that juvenile salmon emigrating later in the season (i.e., late May and June) achieve higher weight gains during their first 90 days of ocean residency.

1. Introduction

Chinook salmon (*Oncorhynchus tshawytscha*) populations vary with ocean climate conditions [*Mantua et al.*, 1997], and unfavorable climate periods can result in low recruitment to the adult population [e.g., *Kruse*, 1998; *Lindley et al.*, 2009]. Chinook salmon spawn in rivers, and after a few months rearing in freshwater, juveniles migrate to the coastal ocean where food supplies and growth prospects are typically greater than in their natal river [*Gross et al.*, 1988]. While there is a great deal of diversity in the timing of aspects of their life history, Chinook salmon juveniles typically migrate to the ocean in spring, presumably to take advantage of the peak in production associated with the onset of coastal upwelling [*Quinn*, 2005]. Feeding conditions experienced by juvenile Chinook salmon in the ocean are highly variable among years, owing to variations in winter preconditioning [*Black et al.*, 2010; *Satterthwaite et al.*, 2012; *Schroeder et al.*, 2013, 2014], and the timing, intensity, and duration of upwelling [*Lindley et al.*, 2009]. This initial period of ocean residency is thought to occur in the region of the natal river [*Mueter et al.*, 2002], and climate and forage conditions largely determine subsequent adult salmon abundance [*Beamish and Mahnken*, 2001; *Wells et al.*, 2012].

Early marine mortality varies as a function of growth and size [*Holtby et al.*, 1990; *Woodson et al.*, 2013], such that slower growing fish have a lower probability of survival when first entering the ocean during less productive conditions. During years of reduced forage biomass, Chinook salmon exhibit poorer condition [*Wells et al.*, 2012] which is linked to increased mortality [*Holtby et al.*, 1990; *Woodson et al.*, 2013] presumably associated with relatively greater predation on smaller fish [*Tucker et al.*, 2013]. Measuring growth of salmon at sea, especially during their first year, is difficult because the size distribution of populations changes in response to both growth and size-dependent mortality, and populations are moving and mixing with other populations. With limited sampling opportunities, developing robust relationships that quantify the spatiotemporal influences of coastal ocean properties on growth of Chinook salmon has therefore remained elusive.

The present work describes a novel approach to identify the effects of environmental conditions and upwelling variability on growth and condition of juvenile Chinook salmon in central California coastal

waters. The method uses a fully coupled ecosystem model consisting of an ocean circulation submodel, a biogeochemical submodel, and an individual-based submodel for juvenile salmon. The overall modeling framework is similar to the end-to-end ecosystem model configuration used by *Fiechter et al.* [2014] to investigate sardine and anchovy population dynamics in the California Current System (CCS). By tracking environmental and feeding conditions experienced by individual fish throughout their life history, the model provides new insight into the impact of physical and biological ocean variability on the growth of juvenile Chinook salmon off central California during their critical first period at sea.

2. Ecosystem Model Framework

2.1. Regional Ocean Circulation Submodel

The ocean circulation submodel is an implementation of the Regional Ocean Modeling System (ROMS) [*Haidvogel et al.*, 2008; *Shchepetkin and McWilliams*, 2005] for the CCS and ranges from 30°N to 48°N and 116°W to 134°W. The grid resolution is set to 1/10° (~10 km) horizontally and comprises 42 nonuniform terrain-following levels vertically. The CCS ROMS model is forced on all lateral boundaries by monthly averaged fields from the Simple Ocean Data Assimilation reanalysis [*Carton et al.*, 2000] to guarantee realistic transport values and temperature and salinity profiles. Surface forcing is derived from the data sets for Common Ocean-Ice Reference Experiments [*Large and Yeager*, 2008] and consists of monthly mean winds, air temperature, sea level pressure, specific humidity, precipitation, and shortwave and downwelling longwave radiation.

2.2. Biogeochemical Submodel

The biogeochemical submodel is based on the 11 component North Pacific Ecosystem Model for Understanding Regional Oceanography (NEMURO) model [*Kishi et al.*, 2007], and specifically parameterized for the CCS region [*Fiechter et al.*, 2014]. NEMURO includes three limiting macronutrients (nitrate, ammonium, and silicic acid), two phytoplankton groups (nanophytoplankton and diatoms), three zooplankton groups (microzooplankton, mesozooplankton, and krill), and three detritus pools (dissolved and particulate organic nitrogen and particulate silica). Coupling to the ocean circulation is done by solving a transport equation in ROMS for each NEMURO variable at every time step. The initial and boundary conditions for nitrate and silicic acid are derived from monthly climatological concentrations (World Ocean Atlas 2001, $1° \times 1°$ horizontal resolution) [*Conkright and Boyer*, 2002]. The initial and boundary conditions for ammonium, phytoplankton, zooplankton, and detritus are set to a small value (0.1 mmolN m^{-3}).

2.3. Individual-Based Submodel for Juvenile Salmon

The individual-based submodel for juvenile salmon includes a bioenergetics model to determine growth and an area-restricted search algorithm to simulate foraging behavior. The bioenergetics model is adapted from the DEBkiss model [*Jager et al.,* 2013], where hourly growth is given by the difference between the biomass assimilated and that expended on maintenance metabolism and swimming; growth is then converted to somatic body mass with a set efficiency (supporting information, equation (1)). Individuals feed at a rate dependent on prey density given by near-surface krill concentrations from the NEMURO submodel. Because feeding requires external resources to be transported internally across a surface (e.g., gut wall), maximum feeding rate is assumed proportional to surface area (supporting information, equation (2)). Prey biomass consumed is converted to assimilated energy with a fixed efficiency. The resource dependence of feeding rate is captured via a scaled hyperbolic functional response depending on the individual's maximum feeding rate, specific search area, and swim speed (supporting information, equations (3) and (4)). Maintenance metabolism represents the cost of metabolic upkeep and varies with temperature and body mass, while activity metabolic costs are assumed to depend on body mass and swim speed (supporting information, equations (5) and (6)). Hence, the swim speed of an individual affects both its metabolic gains via feeding and costs via activity. In the model, juvenile Chinook salmon were assumed to swim at a fixed speed of one body length per second [e.g., *Tanaka et al.*, 2005].

Horizontal movement to mimic foraging behavior is based on depth-averaged krill concentrations from NEMURO and swim speed. Every 3 h, model individuals use an area-restricted search algorithm [*Watkins and Rose*, 2013] to modify their swimming direction and move toward the center of the nearby grid cell (i.e., the cell they currently occupy plus the directly adjacent eight cells) where depth-averaged krill

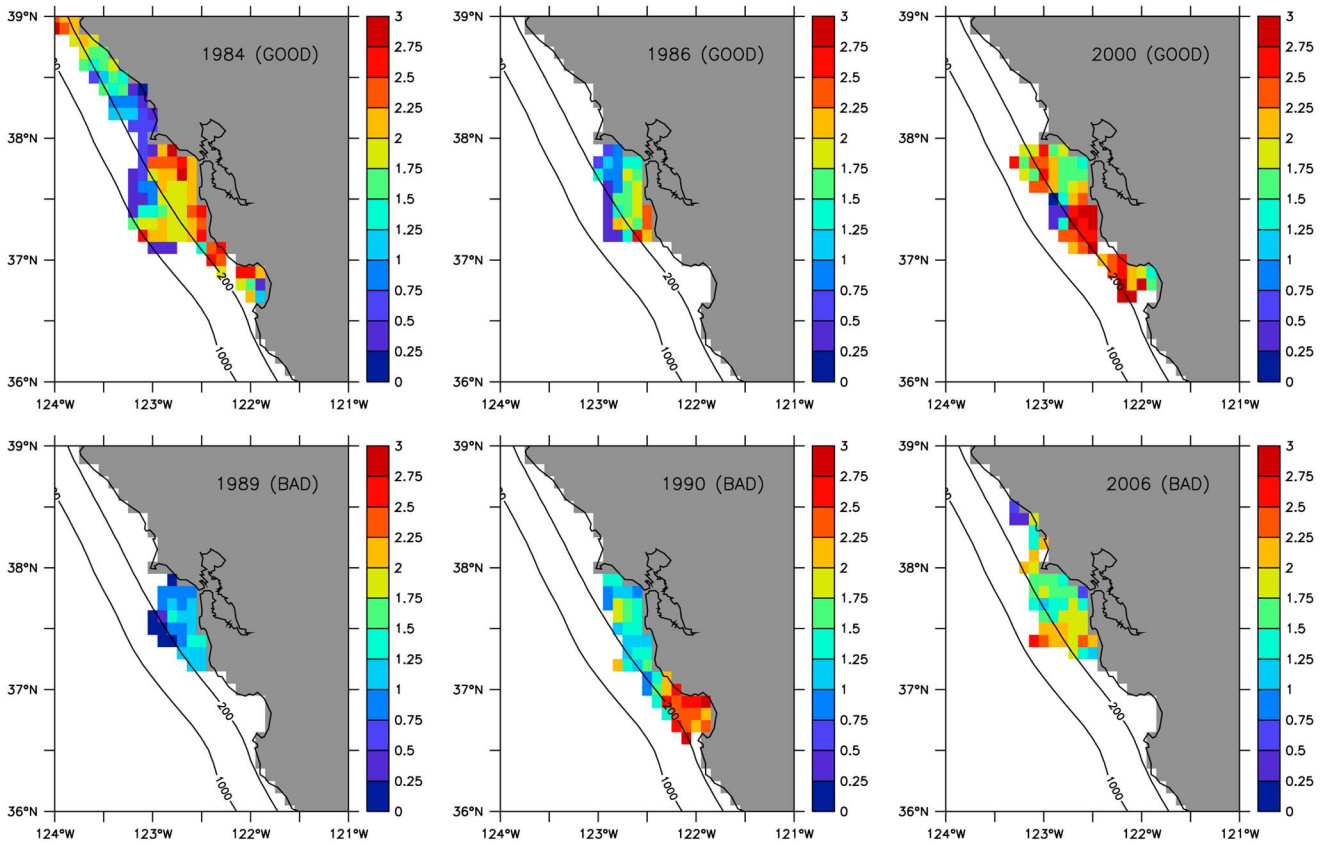

Figure 1. Simulated maximum monthly averaged growth rate (g d^{-1}) for juvenile Chinook salmon over all individuals and times for each grid cell. (top row) Years identified as favorable for survival (1984, 1986, and 2000). (bottom row) Years identified as unfavorable for survival (1989, 1990, and 2006).

concentrations are highest. This behavior allows model individuals to follow horizontal grid-scale (~10 km) gradients of prey availability and swim upgradient toward the neighboring cell with the best feeding potential. The search algorithm is thus equivalent to moving toward the local maximum in depth-averaged krill concentrations by evaluating horizontal gradients in nine discretized directions. While fish in nature presumably encounter environmental patchiness at scales smaller than 10 km (especially in nearshore areas), the search approximation used here is consistent with model individuals being able to sense prey variability at the spatial scales determined by the grid resolution. To introduce spread in foraging patterns, a random deviation normally distributed between −45° and 45° is added to the swimming direction each time movement is updated.

2.4. Model Simulations and Analysis

A series of favorable and unfavorable years were selected a priori based on a virtual population analysis of coastal California salmon stocks conducted by *Kilduff et al.* [2014] in which historical fish quantities for a given age were reconstructed based on fisheries and natural mortality estimates. The years considered here correspond to the three best (1984, 1986, and 2000) and worst (1989, 1990, and 2006) survival years for California Chinook salmon populations. The ecosystem model was then run for each of the six years to determine if the simulations could identify favorable or unfavorable growth conditions for juvenile salmon and relate them to potential environmental drivers affecting feeding success.

A total of 2000 model individuals were released into the Gulf of the Farallones (GOF) at the San Francisco Bay outlet (~37.8°N, 122.5°W) every 5 days from the beginning of April to the end of June (i.e., the primary timing of California Chinook salmon emigration to sea) [*Satterthwaite et al.*, 2014] and followed until the end of the calendar year. Individuals that entered the domain had identical attributes regardless of emigration time, with a weight of 7.4 g and a length of 87.1 mm [*MacFarlane*, 2010]. The simulations were used to predict

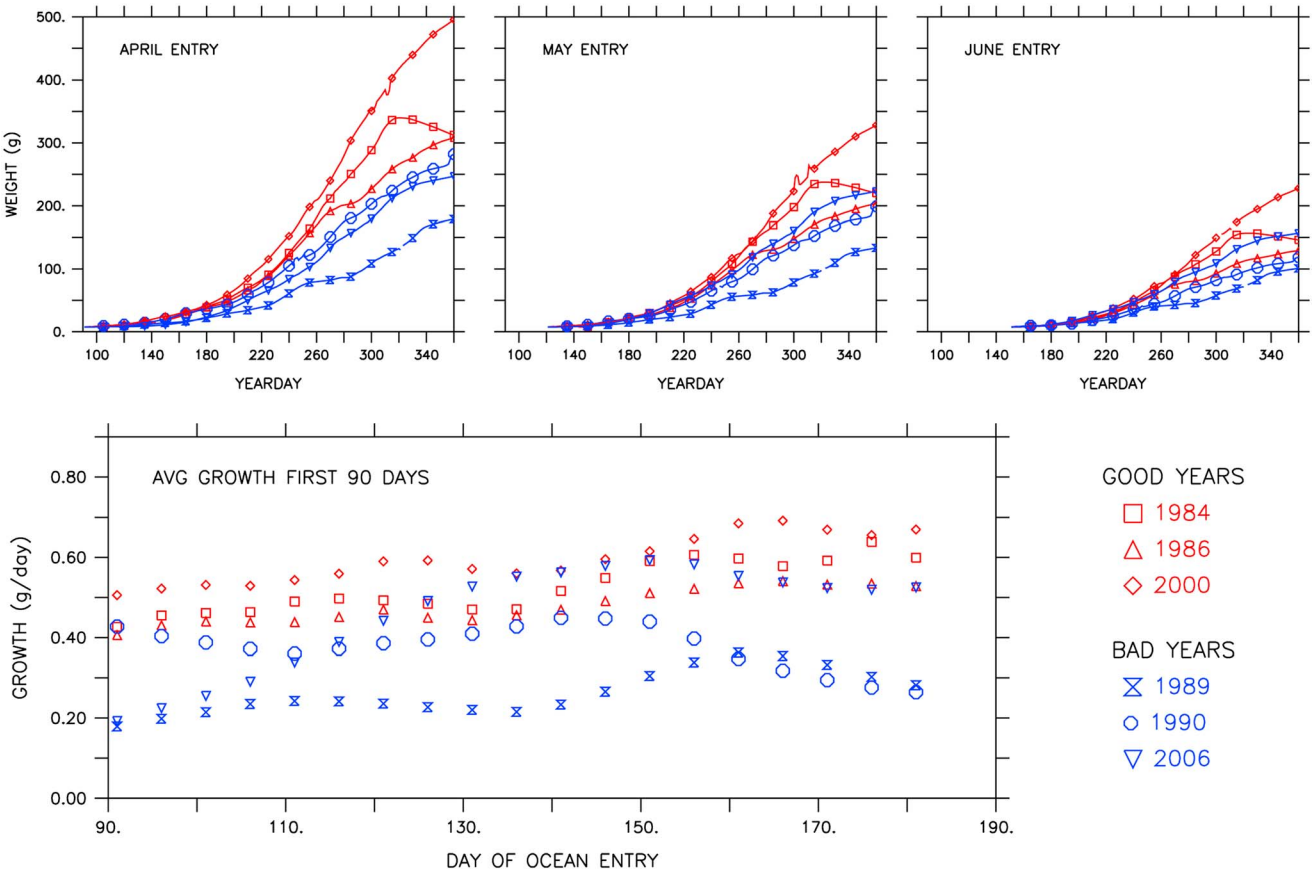

Figure 2. Simulated growth for juvenile Chinook salmon as a function of year and date of ocean entry. (top row) Weight (g) versus time (yearday) relationship following ocean entry in April, May, and June (left to right). (bottom) Average growth rate (g d^{-1}) during first 90 days at sea as a function of ocean entry day. Red (blue) curves and symbols denote years identified as favorable (unfavorable) for survival.

daily and monthly averaged growth rates for individuals released during the same calendar month or present within the same grid cell, and to generate a consistent set of prey concentration, temperature, and upwelling-related metrics that could explain year-to-year differences in growth conditions.

3. Results

3.1. Juvenile Salmon Distribution and Growth

Model individuals were present in the GOF for all years, and their distributions extended to the north in 1984 and 2006 and to the south in 1990 and 2000 (Figure 1), which suggests that latitudinal spread from the point of ocean entry was not consistent among favorable or unfavorable years. In contrast to distributions, simulated maximum monthly growth rates were more distinct among years, with local values up to 3 g d^{-1} in 1984 and 2000 (favorable years) and below 1 g d^{-1} in 1989 (unfavorable year). However, the results also indicated substantial along-shelf variability in growth conditions for each year, as evidenced by local rates in 1990 (unfavorable year) mainly below 1.5 g d^{-1} near the point of ocean entry in the GOF but above 2 g d^{-1} farther to the south near Monterey Bay.

As a direct result of higher growth rates during favorable years, model individuals reached a maximum body mass nearly twice that achieved under unfavorable conditions (e.g., 300–500 g versus 150–250 g for ocean entry in April) (Figure 2, top row). The simulations also suggest that, among unfavorable years, 1989 was particularly extreme, with juvenile salmon released in April only reaching a maximum body mass of ~150 g versus ~250 g in 1990 and 2006. Similarly, while 1984 and 2000 emerged as particularly positive years, overall simulated growth rates were comparable for 1986 (favorable year) and 1990 (unfavorable year) for

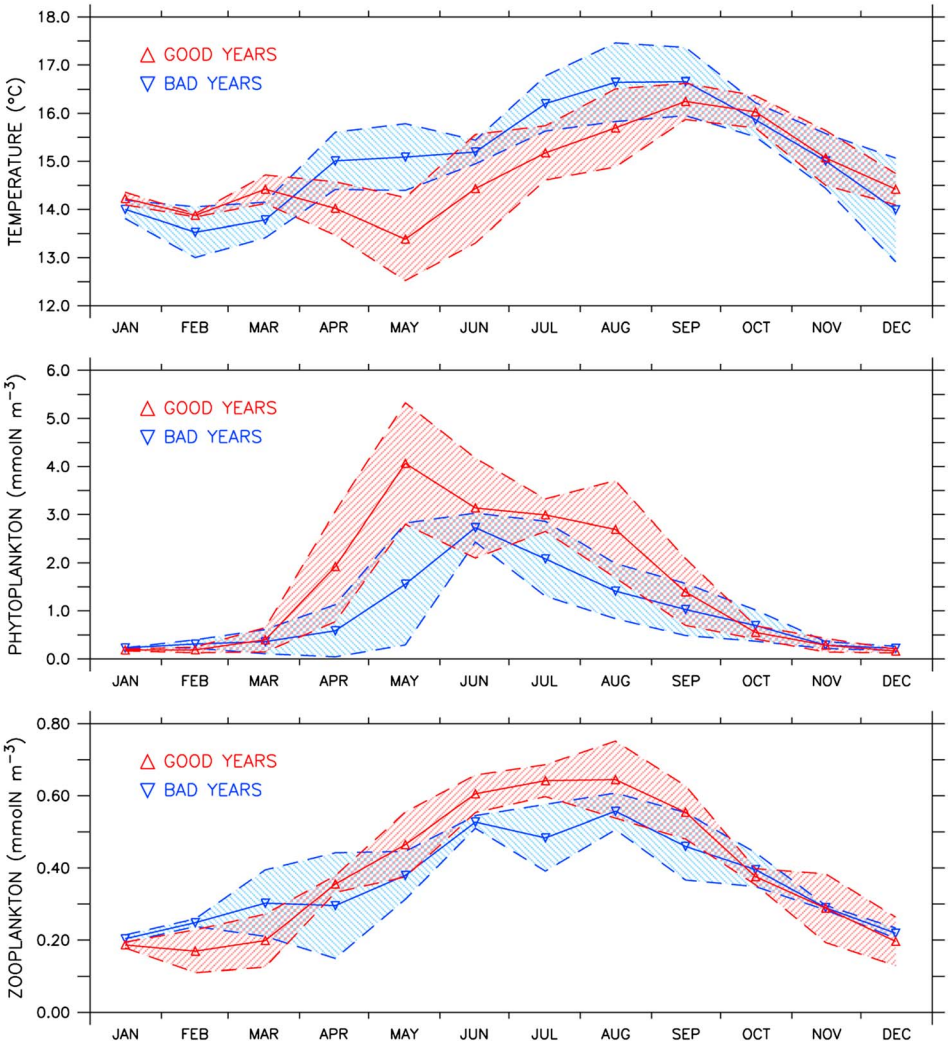

Figure 3. Simulated environmental conditions in the Gulf of the Farallones for years identified as favorable (1984, 1986, and 2000; red) and unfavorable (1989, 1990, and 2006; blue) for juvenile Chinook salmon survival. (top) Sea surface temperature (°C). (middle) Surface large phytoplankton (diatom) concentration (mmolN m^{-3}). (bottom) Surface krill concentration (mmolN m^{-3}). Solid lines denote mean value, and dashed lines indicate ± 1 standard deviation.

individuals entering the ocean in May and June. Simulated mean growth rates during the first 90 days following ocean entry were moderately higher for individuals emigrating later in the season (i.e., late May and June), except in 1990 when rates decreased by about half (Figure 2, bottom). However, the growth rate advantage experienced by later migrating fish did not compensate for the shorter available growing season, such that late migrants were substantially smaller at the end of the year than early migrants.

3.2. Environmental Conditions Favoring Growth

Based on monthly mean ROMS and NEMURO fields averaged spatially over the GOF (i.e., between 37.25 and 38°N and out to the 1000 m isobath), years that were identified a priori as favorable for salmon survival generally exhibited cooler sea surface temperatures and higher phytoplankton concentrations during spring (March–May) (Figure 3, top and middle), which resulted in higher krill concentrations during summer (June–August) (Figure 3, bottom). Years leading to higher juvenile salmon growth in the model, thus, coincided with the occurrence of enhanced coastal upwelling earlier in spring. However, the relatively large spread (i.e., standard deviation) around mean surface temperatures and phytoplankton concentrations during spring for favorable years also indicate that different upwelling conditions may lead to similar growth rates. Spatial differences in simulated growth rates (see Figure 1) suggest that foraging

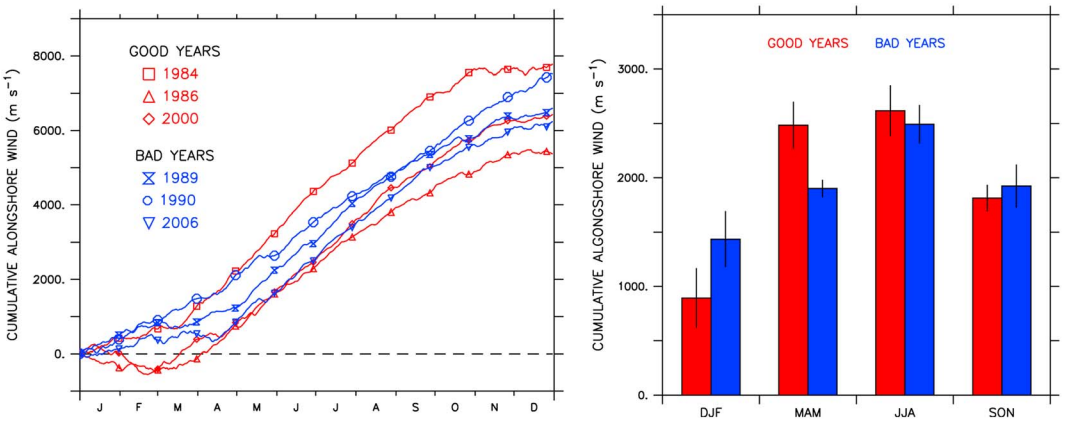

Figure 4. Cumulative alongshore wind ($m\,s^{-1}$) at 37°N and 100 km offshore for years identified as favorable (1984, 1986, and 2000; red) and unfavorable (1989, 1990, and 2006; blue) for juvenile Chinook salmon survival; wind values are defined as positive when upwelling is favorable (i.e., equatorward). (left) Cumulative wind. (right) Cumulative wind summed by season (DJF: December-January-February; MAM: March-April-May; JJA: June-July-August; and SON: September-October-November). For each season, colored bars represent mean value, and error bars indicate ± 1 standard deviation.

conditions in the GOF may be dictated by a balance between upwelling intensity and offshore/alongshore advection, where weaker upwelling would result in lower biological production but higher local retention (e.g., 1984), while stronger upwelling would lead to higher biological production but lower local retention (e.g., 2000).

The relationship between enhanced spring upwelling and juvenile salmon growth was further evidenced by inspecting cumulative alongshore winds offshore of the GOF (Figure 4, left). Alongshore wind is a proxy for total upwelling intensity similar to that defined by *Bograd et al.* [2009] and based on the Bakun upwelling index. Based on the model simulations, neither the date of the spring transition, length of the upwelling season, nor total cumulative upwelling emerged as reliable proxies for environmental conditions favoring juvenile salmon growth (Table 1). In fact, two of the years for which juvenile salmon growth was identified as favorable (i.e., 1986 and 2000) exhibited later spring transition days, and thus shorter overall upwelling seasons. In contrast, mean upwelling intensity (i.e., slope of cumulative alongshore wind) during the first half of the season was significantly greater during years favoring growth ($p = 0.01$) (Table 1). The relationship between growth conditions and early season upwelling intensity was also demonstrated more directly by considering cumulative alongshore wind patterns by season, with favorable years clearly standing out during spring (March–May) compared to winter (December–February), summer (June–August), and fall (September–November) (Figure 4, right).

Table 1. Cumulative Alongshore Wind Characteristic at 37°N and 100 km Offshore (See Figure 4)[a]

	Favorable Years			Unfavorable Years		
Explanatory Variable	1984	1986	2000	1989	1990	2006
Spring transition (yearday)	1	52	58	1	1	6
Duration of upwelling season (days)	365	295	308	365	364	360
Total cumulative alongshore wind ($10^6\,m\,s^{-1}$)	6.02	3.10	4.09	4.72	5.18	4.10
Total cumulative wind intensity ($m\,s^{-1}\,d^{-1}$)	21.3	20.5	22.4	18.1	20.7	17.6
Early cumulative wind intensity[b] ($m\,s^{-1}\,d^{-1}$)	24.3	23.4	25.9	16.5	19.7	15.5

[a]Spring transition is defined as the minimum of cumulative wind curve; duration of upwelling season is defined as number of days between spring transition and maximum of cumulative wind curve; total cumulative upwelling is defined as cumulative wind values summed over upwelling season; Total (early) cumulative wind intensity is defined as average slope of cumulative wind curve over the entire (first half of) upwelling season.
[b]Early cumulative wind intensity was significantly different between favorable and unfavorable years ($p = 0.01$).

4. Discussion

The present study illustrates how results from a fully coupled physical-biogeochemical-fish model can be used to gain insight into the environmental conditions impacting the growth of juvenile Chinook salmon off central California during their critical early period at sea. Despite simplifications in the biogeochemical (e.g., neglecting krill vertical migration) and individual-based (e.g., simplified foraging behavior based solely on local prey density gradients) submodels, simulated growth rates are similar to previously reported values for juvenile Chinook salmon off central California. Including both favorable and unfavorable survival years, average growth rates in the model are $0.69 \pm 0.35\,g\,d^{-1}$ for June–August and $1.41 \pm 0.28\,g\,d^{-1}$ for September–November, compared to observed values of 0.79 and $1.47\,g\,d^{-1}$ for approximately the same periods [*MacFarlane*, 2010].

Based on the model solutions, years favorable for juvenile salmon survival off central California are characterized by particularly intense early season upwelling (i.e., March–May), leading to enhanced krill concentrations and higher growth rates in the GOF during summer. This finding is consistent with the correlations between early spring isopycnal depth and summer krill populations reported by *Schroeder et al.* [2014] for the same region. The cascading effect from regions of enhanced upwelling to primary productivity and krill abundances is also known to cause substantial patchiness in habitat characteristics between the GOF and Monterey Bay [*Santora et al.*, 2014]. Spatial variability in simulated growth patterns for juvenile salmon within and across years provides evidence for latitudinal changes in habitat quality that may be associated with a balance between upwelling intensity and offshore/alongshore advection [*Santora et al.*, 2011].

With regard to timing of emigration, model individuals entering the ocean later in the season (i.e., late May and June) typically achieve higher growth rates during their first 90 days at sea, which is in agreement with the end of May optimal release timing identified by *Satterthwaite et al.* [2014] using tagged salmon hatchery data. Furthermore, early growth potential in the model remains high (low) for good (bad) years throughout the period of ocean immigration (i.e., April–June), except for 2006 when model individuals entering the ocean early (late) grew at rates characteristic of poor (good) environmental conditions (see Figure 2). In this particular case, simulated upwelling intensity in 2006 was weak in March (i.e., "bad year" criterion) but increased to "good year" levels during April–June (see Figure 3). Under such circumstances, the timing of ocean emigration would play an important role in determining overall juvenile growth and survival for that year.

While the simulations did not establish a clear within-year relationship between spring transition date and optimal growth conditions [*Satterthwaite et al.*, 2014], the spring transition is less consistently identifiable at 37°N (this study) than at 39°N [*Satterthwaite et al.*, 2014] because of more persistent year-round upwelling conditions at 37°N. In fact, the model results suggest that, based on alongshore wind properties directly offshore of the GOF, none of the standard metrics based on cumulative upwelling [*Bograd et al.*, 2009] provides a useful proxy for distinguishing between favorable and unfavorable growth conditions.

It should be emphasized that the results presented here depend, to some extent, on the fact that horizontal foraging for model individuals was solely based on maximizing growth by swimming toward regions of higher prey availability. While oceanic dispersal of California Central Valley Chinook salmon presumably evolved in response to improved growth potential in persistently productive marine waters, a reasonable short-term objective for salmon during dispersal is to make movement decisions that maximize their growth rate (i.e., the movement toward higher prey concentrations used in the present simulations) as mortality rates are thought to be largely size dependent [*Cross et al.*, 2009; *Woodson et al.*, 2013]. An improved understanding of the tension between local growth and larger-scale dispersal may be obtained via statistical models that quantify relationships between juvenile salmon survival and ocean conditions at diverse spatiotemporal scales. Knowledge gained from salmon distribution analyses that include spatially explicit environmental covariates and prey resources could greatly increase model realism by providing a consistent set of cues (or optimal conditions) to inform the movement rules prescribed in the individual-based submodel [e.g., *Burke et al.*, 2013]. Future simulations should also explore the impact of predation mortality on feeding behavior (i.e., trade-off between maximizing growth and avoiding predation). However, adding explicit predation mortality would require sufficient knowledge on how predation rates vary in the ocean with size and realistic hypotheses on how fish change foraging strategies as they grow.

Finally, while not yet ready for management applications, the ecosystem model described here provides a comprehensive framework for explicitly studying the wide array of mechanisms affecting juvenile salmon

growth following ocean emigration and may in the future offer higher predictive power than more traditional forecasting approaches based on climate indices or other ad hoc proxies for ecosystem productivity.

Acknowledgments
This research was supported by the following grants: NA10OAR4320156 funded by the NOAA Fisheries Office of Science and Technology and the NOAA Office of Oceanic and Atmospheric Research (Climate Program Office), N000141210893 funded by the Office of Naval Research Marine Mammals and Biology Program, and NNX11AP11G-003 funded by NASA Applied Sciences. The authors thank J. Field, E. Danner, N. Mantua, M. Henderson, S. Hayes, and B. Burke for helpful discussions and reviews. Insightful comments from one anonymous reviewer are also acknowledged. The model output used for this study can be obtained by contacting the lead author directly.

The Editor thanks an anonymous reviewer for assisting in the evaluation of this paper.

References

Beamish, R. J., and C. Mahnken (2001), A critical size and period hypothesis to explain natural regulation of salmon abundance and the linkage to climate and climate change, *Prog. Oceanogr.*, *49*, 423–435.

Black, B. A., I. D. Schroeder, W. J. Sydeman, S. J. Bograd, and P. W. Lawson (2010), Wintertime ocean conditions synchronize rockfish growth and seabird reproduction in the central California Current ecosystem, *Can. J. Fish. Aquat. Sci.*, *67*(7), 1149–1158.

Bograd, S. J., I. Schroeder, N. Sarkar, X. Qiu, W. J. Sydeman, and F. B. Schwing (2009), Phenology of coastal upwelling in the California Current, *Geophys. Res. Lett.*, *36*, L01602, doi:10.1029/2008GL035933.

Burke, B. J., M. C. Liermann, D. J. Teel, and J. J. Anderson (2013), Environmental and geospatial factors drive juvenile Chinook salmon distribution during early ocean migration, *Can. J. Fish. Aquat. Sci.*, *70*(8), 1167–1177.

Carton, J. A., G. Chepurin, and X. Cao (2000), A Simple Ocean Data Assimilation analysis of the global upper ocean 1950–1995 Part 2: Results, *J. Phys. Oceanogr.*, *30*, 311–326.

Conkright, M. E., and T. P. Boyer (2002), World Ocean Atlas 2001: Objective analyses, data statistics, and figures, CD-ROM Documentation, 17 pp., Natl. Oceanogr. Data Cent., Silver Spring, Md.

Cross, A. D., D. A. Beauchamp, J. H. Moss, and K. W. Myers (2009), Interannual variability in early marine growth, size-selective mortality, and marine survival for Prince William Sound pink Salmon, *Mar. Coast. Fish.*, *1*(1), 57–70.

Fiechter, J., K. A. Rose, E. N. Curchitser, and K. Hedstrom (2014), The role of environmental controls in determining sardine and anchovy population cycles in the California Current: Analysis of an end-to-end model, *Prog. Oceanogr.*, doi:10.1016/j.pocean.2014.11.013.

Gross, M. R., R. M. Coleman, and R. M. McDowall (1988), Aquatic productivity and the evolution of diadromous fish migration, *Science*, *239*, 1291–1293.

Haidvogel, D. B., et al. (2008), Ocean forecasting in terrain-following coordinates: Formulation and skill assessment of the Regional Ocean Modeling System, *J. Comput. Phys.*, *227*, 3595–3624, doi:10.1016/j.jcp.2007.06.016.

Holtby, L. B., B. C. Anderson, and R. K. Kadowaki (1990), Importance of smolt size and early ocean growth to interannual variability in marine survival of coho salmon (*Oncorhynchus kisutch*), *Can. J. Fish. Aquat. Sci.*, *47*, 2181–2194.

Jager, T., B. T. Martin, and E. I. Zimmer (2013), DEBkiss or the quest for the simplest generic model of animal life history, *J. Theor. Biol.*, *328*, 9–18, doi:10.1016/j.jtbi.2013.03.011.

Kilduff, D. P, L. W. Botsford, and S. L. H. Teo (2014), Spatial and tmeporal covariability in early ocean survival of Chinook salmon (Oncorhynchus tshawytscha) along the west coast of North America, *ICEA J. Mar. Sci.*, doi:10.1093/icesjms/fsu031.

Kishi, M. J., et al. (2007), NEMURO—A lower trophic level model for the North Pacific marine ecosystem, *Ecol. Modell.*, *202*, 12, doi:10.1016/j.ecolmodel.2006.08.021.

Kruse, G. H. (1998), Salmon run failures in 1997-1998: a link to anomalous ocean conditions?, *Alaska Fishery Res. Bull.*, *5*, 55–63.

Large, W. G., and S. G. Yeager (2008), The global climatology of an interannually varying air-sea flux data set, *Clim. Dyn.*, *33*, 341–363, doi:10.1007/s00382-0008-0441-3.

Lindley, S. T., et al. (2009), What caused the Sacramento River fall Chinook salmon stock collapse?, NOAA Tech Memo NMFS-SWFSC 447.

MacFarlane, R. B. (2010), Energy dynamics and growth of Chinook salmon (*Oncorhynchus tshawytscha*) from the Central Valley of California during the estuarine phase and first ocean year, *Can. J. Fish. Aquat. Sci.*, *67*, 1549–1565, doi:10.1139/F10-080.

Mantua, N. J., S. R. Hare, Y. Zhang, J. M. Wallace, and R. C. Francis (1997), A Pacific decadal climate oscillation with impacts on salmon, *Bull. Am. Meteorol. Soc.*, *78*, 1069–1079.

Mueter, F. J., R. M. Peterman, and B. J. Pyper (2002), Opposite effects of ocean temperature on survival rates of 120 stocks of Pacific salmon (Oncorhynchus spp.) in northern and southern areas, *Can. J. Fish. Aquat. Sci.*, *59*, 456–463.

Quinn, T. P. (2005), The behavior and ecology of Pacific salmon and trout, 388 pp., Univ. of Washington Press, Bethesda.

Santora, J. A., W. J. Sydeman, I. D. Schroeder, B. K. Wells, and J. C. Field (2011), Mesoscale structure and oceanographic determinants of krill hotspots in the California Current: Implications for trophic transfer and conservation, *Prog. Oceanogr.*, *91*, 397–409, doi:10.1016/j.pocean.2011.04.002.

Santora, J. A., I. D. Schroeder, J. C. Field, B. K. Wells, and W. J. Sydeman (2014), Spatio-temporal dynamics of ocean conditions and forage taxa reveals regional structuring of seabird-prey relationships, *Ecol. Appl.*, *1891*, doi:10.1890/1813-1605.

Satterthwaite, W. H., M. S. Mohr, M. R. O'Farrell, and B. K. Wells (2012), A Bayesian hierarchical model of size-at-age in ocean-harvested stocks—Quantifying effects of climate and temporal variability, *Can. J. Fish. Aquat. Sci.*, *69*(5), 942–954.

Satterthwaite, W. H., S. M. Carlson, S. Vincenzi, S. D. Allen-Moran, S. J. Bograd, and B. K. Wells (2014), Match-mismatch dynamics and the relationship between ocean-entry timing and relative ocean recovery rates of Central Valley fall run Chinook salmon, *Mar. Ecol. Prog. Ser.*, *511*, 237–248.

Schroeder, I. D., E. Hazen, B. A. Black, S. J. Bograd, W. J. Sydeman, J. Santora, and B. K. Wells (2013), The North Pacific High and wintertime pre-conditioning of California Current productivity, *Geophys. Res. Lett.*, *40*, 541–546, doi:10.1002/grl.50100.

Schroeder, I. D., J. A. Santora, A. M. Moore, C. A. Edwards, J. Fiechter, E. L. Hazen, S. J. Bograd, J. C. Field, and B. K. Wells (2014), Application of a data-assimilative regional ocean modeling system for assessing California Current System ocean conditions, krill, and juvenile rockfish interannual variability, *Geophys. Res. Lett.*, *41*, 5942–5950, doi:10.1002/2014GL061045.

Shchepetkin, A. F., and J. C. McWilliams (2005), The regional oceanic modeling system (ROMS): A split-explicit, free-surface, topography-following-coordinate oceanic model, *Ocean Model.*, *9*, 347–404.

Tanaka, H., Y. Naito, N. D. Davis, S. Urawa, H. Ueda, and M. Fukuwaka (2005), First record of the at-sea swimming speed of a Pacific salmon during its oceanic migration, *Mar. Ecol. Prog. Ser.*, *291*, 307–312.

Tucker, S., M. Hipfner, J. R. Candy, C. Wallace, T. D. Beacham, and M. Trudel (2013), Stock-specific predation of Rhinoceros Auklets (*Cerorhinca monocerata*) on juvenile salmon in Coastal British Columbia, North Pacific Anadromous Fisheries Commission, *Tech. Rep. No. 9: 95-96*.

Watkins, K. S., and K. A. Rose (2013), Evaluating the performance of individual-based animal movement models in novel environments, *Ecol. Modell.*, *250*, 214–234.

Wells, B. K., J. A. Santora, J. C. Field, R. B. MacFarlane, B. B. Marinovic, and W. J. Sydeman (2012), Population dynamics of Chinook salmon *Oncorhynchus tshawytscha* relative to prey availability in the central California coastal region, *Mar. Ecol. Prog. Ser.*, *457*, 125–137.

Woodson, L. E., B. K. Wells, P. K. Weber, R. B. MacFarlane, G. E. Whitman, and R. C. Johnson (2013), Size, growth, and origin-dependent mortality of juvenile Chinook salmon *Oncorhynchus tshawytscha* during early ocean residence, *Mar. Ecol. Prog. Ser.*, *487*, 163–175.